Magnetic Resonance in Medicine 64:186–193 (2010)

High-Performance Computing MRI Simulations

Tony Stöcker,[1,2]* Kaveh Vahedipour,[1] Daniel Pflugfelder,[1] and N. Jon Shah[1–3]

A new open-source software project is presented, JEMRIS, the Jülich Extensible MRI Simulator, which provides an MRI sequence development and simulation environment for the MRI community. The development was driven by the desire to achieve generality of simulated three-dimensional MRI experiments reflecting modern MRI systems hardware. The accompanying computational burden is overcome by means of parallel computing. Many aspects are covered that have not hitherto been simultaneously investigated in general MRI simulations such as parallel transmit and receive, important off-resonance effects, nonlinear gradients, and arbitrary spatio-temporal parameter variations at different levels. The latter can be used to simulate various types of motion, for instance. The JEMRIS user interface is very simple to use, but nevertheless it presents few limitations. MRI sequences with arbitrary waveforms and complex interdependent modules are modeled in a graphical user interface–based environment requiring no further programming. This manuscript describes the concepts, methods, and performance of the software. Examples of novel simulation results in active fields of MRI research are given. Magn Reson Med 64:186–193, 2010. © 2010 Wiley-Liss, Inc.

Key words: MRI simulation; Bloch equations; sequence development; high performance computing; object-oriented design patterns

Numerical simulation of MRI experiments, based on the Bloch equation, is an essential tool for a variety of different research directions. In the field of pulse sequence optimization, e.g., for artifact detection and elimination, simulations allow one to differentiate between effects arising principally from MRI physics and those due to hardware imperfections. Another prominent application is the design of specialized radiofrequency (RF) pulses. In general, the interpretation and validation of experimental results benefits from comparisons to simulated data. Many more applications possibly add to this list, not to forget that controlled numerical MRI experiments are also valuable for educational purposes.

In its most general form, numerical simulation of an MRI experiment is a demanding task. This is due to the fact that a huge spin ensemble has to be simulated in order to obtain realistic results. To overcome this, several published approaches reduce the problem size in different ways. The most prominent method is to consider analytical solutions of the problem (1–3). In cases of simultaneous RF excitation and time-varying gradient fields, no general analytical solution exists and, thus, the important field of selective excitation cannot be studied with analytical approaches. In the past, numerical solutions have also been considered (4,5) but hardware and software architectures pertaining at that time limited simulations to small spin systems with reduced flexibility in setup and extensibility of the numerical experiments. Apart from the computational demand, the complexity of the MRI imaging sequence is also an obstacle. A multipurpose MRI simulation environment should provide functionality for rapid-sequence prototyping; otherwise, it will be of limited interest only. However, providing an easy-to-use framework should by no means increase the internal complexity thereof. This would reduce the possibility of extending and changing the framework and again result in limited usability for tailored applications.

The Jülich Extensible MRI Simulator (JEMRIS) project was initiated, taking all of the aforementioned considerations into account. The present manuscript summarizes the functionality of the framework, provides performance benchmarks, and shows applications in currently active research areas such as nonlinear spatially encoding fields, parallel transmit RF pulse design, and compressed sensing of moving objects.

Concepts

General Features

The original driving forces for JEMRIS were (i) the need for accurate MRI simulations in the most general case of noninteracting classic spins (e.g., for the design of long RF pulses, where, simultaneously, gradient fields and relaxation need to be taken into account); (ii) the availability of high-performance computing at the authors' institution; and (iii) the lack of a freely available software project capable of the following fundamental features, which are now supported by JEMRIS:

1. Utilizing an optimized library for numerical solutions of differential equations provides accurate three-dimensional MRI simulation results in cases where no analytical solution is available, e.g., to simulate complex nonlinear RF waveforms for selective excitation or adiabatic full passage pulses.
2. JEMRIS can deal with arbitrary RF and gradient waveforms, arbitrary multichannel Tx-Rx coil geometries and configurations, as well as many important physical concepts, such as nonlinear gradients, chemical shift, reversible spin dephasing (T_2^*), susceptibility-induced off-resonance, temporal varying

[1]Institute of Neuroscience and Medicine-4, Juelich, Germany.
[2]JARA–Translational Brain Medicine, Germany, Juelich and Aachen.
[3]Department of Neurology, RWTH Aachen University, Aachen, Germany.
*Correspondence to: Tony Stöcker, Ph.D., Institute of Neuroscience and Medicine-4, Forschungszentrum Jülich GmbH, 52425 Jülich, Germany. E-mail: t.stoecker@fz-juelich.de

Received 3 July 2009; revised 15 January 2010; accepted 15 January 2010.
DOI 10.1002/mrm.22406
Published online in Wiley InterScience (www.interscience.wiley.com).

processes of the object (e.g., movement or flow), and concomitant gradient fields.
3. Symbolic mathematical calculations are supported by means of a dedicated library. Thus, many extensions are readily available, with no additional programming involved.
4. The core simulation routines take advantage of massive parallel processing and are available on different hardware architectures. JEMRIS simulations scale on single-core hardware, small high-performance computing clusters, and also on massively parallel supercomputers.
5. A graphical user interface (GUI) is provided with which all simulation parameters are configured, including nearly arbitrary complex MRI sequences.
6. JEMRIS is open source and the community is encouraged to make contributions to the project under www.jemris.org. It has been successfully tested on Linux, Windows, and Mac OS X.

Most important is the first point: in contrast to other currently available MRI simulators, JEMRIS offers a highly optimized computational platform for the most general numerical solution of the Bloch equations of noninteracting classic spins. Further, items 2 and 3 in the above list are not fully covered by other MRI simulators, to the best knowledge of the authors.

Whereas the advantage of including physical concepts such as parallel transmit and receive into MRI simulations is obvious, the benefit of including symbolic mathematical evaluation may not be directly clear. Here, the key feature is that JEMRIS does not provide predefined MRI sequences and experimental setups; for instance, a specialized module for slice selection does not exist. Instead, a few basic building modules exist with high flexibility in parameterization and module interaction. This is achieved by object state observation and crosstalk. Arbitrary parameter dependences may be defined through analytical formulas, which are evaluated by a symbolic math library at runtime. Thus, by means of a dedicated GUI, which requires no further programming, rapid prototyping of almost any new sequence that an ambitious MRI physicist might think of is possible.

Physical Background

The simulator is based on a classic description of MRI physics as described by the Bloch equations. A mathematical and numerical treatment is greatly simplified in the rotating frame of reference. Here, the magnetic field at time t and position $\vec{r}$ is modeled by

$$\vec{B}(\vec{r},t) = [\vec{G}(t)\cdot\vec{r} + B_{NLG}(\vec{r},t) + \Delta B_0(\vec{r},t)]\vec{e}_z + \sum_{n=1}^{N}(B^n_{1x}(\vec{r},t)\vec{e}_x + B^n_{1y}(\vec{r},t)\vec{e}_y) \quad [1]$$

where $\{\vec{e}_x,\vec{e}_y,\vec{e}_z\}$ denote the unit Cartesian vectors and $B^n_{1x,y}(\vec{r},t)$ are the excitation RF components of the nth transmit coil. Spatial dependence accounts for the sensitivity of the coils. In direction of the main field, $\vec{e}_z$, additionally to the linear gradient field, $\vec{G}(t)\cdot\vec{r}$, arbitrary nonlinear gradient (NLG) terms, $B_{NLG}(\vec{r},t)$, can be modeled in JEMRIS. The term $\Delta B_0(\vec{r},t)$ accounts for important off-resonance effects

$$\Delta B_0(\vec{r},t) = \gamma\Delta\omega_{CS}(\vec{r},t) + \gamma\Delta\omega_{Rnd}(\vec{r},t) + \Delta B_{Mac}(\vec{r},t) + \Delta B_{CF}(\vec{r},t) \quad [2]$$

comprising chemical shift ($\Delta\omega_{CS}$), random mesoscopic frequency fluctuations ($\Delta\omega_{Rnd}$), macroscopic field variations (ΔB_{Mac}), and concomitant gradient fields (ΔB_{CF}), respectively. These quantities are discussed below in more detail. The numerical integration of a dynamic system is demanding, if the solution changes rapidly as the oscillating Cartesian components of the transverse magnetization in MRI. Instead, the formulation of the Bloch equation in cylindrical coordinates, $\{M_r,\ \phi,\ M_z\}$, is well suited for numerical implementation:

$$\frac{d}{dt}\begin{pmatrix} M_r \\ \varphi \\ M_z \end{pmatrix} = \begin{pmatrix} \cos\varphi & \sin\varphi & 0 \\ -\frac{\sin\varphi}{M_r} & \frac{\cos\varphi}{M_r} & 0 \\ 0 & 0 & 1 \end{pmatrix} \cdot \left[\begin{pmatrix} -1/T_2 & \gamma B_z & -\gamma B_y \\ -\gamma B_z & -1/T_2 & \gamma B_z \\ \gamma B_y & -\gamma B_x & -1/T_1 \end{pmatrix} \cdot \begin{pmatrix} M_r\cos\varphi \\ M_r\sin\varphi \\ M_z \end{pmatrix} + \begin{pmatrix} 0 \\ 0 \\ M_0/T_1 \end{pmatrix} \right] \quad [3]$$

Equation 3 is solved individually at every position in the object with physical properties

$$P(\vec{r},t) = \{M_0(\vec{r},t), T_1(\vec{r},t), T_2(\vec{r},t), T_2^*(\vec{r},t), \Delta\omega(\vec{r},t), \chi(\vec{r},t)\} \quad [4]$$

where χ indicates the magnetic susceptibility and T_2^* denotes a mesoscopic effective transverse relaxation time which is related to $\Delta\omega_{Rnd}$, as shown later. Multiple isochromats at the same location may be used, e.g., for the simulation of single-voxel MR spectroscopy. The time dependence in Eq. 4 denotes the explicit possibility of specifying time-varying effects such as subject movement. The MR signal of the nth receiver coil, $S_n(t)$, is obtained by integrating all transverse components over the coil volume V

$$S_n(t) \propto \int_V C_n(\vec{r})M_r(\vec{r},t)\exp[i\varphi(\vec{r},t)]d^3r \quad [5]$$

where $C_n(\vec{r})$ denotes the sensitivity of the nth receiver coil. In order to simulate realistic MR signals, processes of different physical nature need to be considered. These effects result in possibly temporally and spatially varying off-resonance conditions of the spin system. First, the well-known T_2^* effect is based on the fact that a real sample will always distort the magnetic field on mesoscopic scales of neighboring isochromats. This effect is simulated by adding small Lorentzian distributed random off-resonance frequency terms to each simulated isochromat, given by the inverse Cauchy-Lorentz cumulative distribution function:

$$\Delta\omega(\vec{r}) = \frac{1}{T_2'}\tan\left[\pi\left(X(\vec{r}) - \frac{1}{2}\right)\right] \quad [6]$$

Here, X denotes a uniformly distributed random variable, $X \in [0,1]$, and T_2' is the user-defined reversible component of the effective relaxation rate, i.e., $1/T_2^* = 1/T_2 + 1/T_2'$. The corresponding dephasing of isochromats leads to an exponentially reversible signal decay, which can be refocused with a spin echo.

Randomness is also introduced to the static spatial positions of the isochromats, which are most conveniently defined on a Cartesian grid. In JEMRIS, the spatial positions are subject to small random variations in the preparation stage because the regular positioning of isochromats on a grid may lead to unrealistic results (6).

Macroscopic field variations, ΔB_{Mac}, may be externally calculated and optionally added to the simulation. Here, subject-induced field inhomogeneities resulting from a susceptibility distribution, $\chi(\vec{r})$, are taken into account by a rapid Fourier-based solution of the Laplace equation (7). Since the method is extremely fast, it is not part of the main high-performance computing program but directly computed within the GUI. Further, off-resonances may occur due to the so-called concomitant fields, ΔB_{CF}, coming from the fact that the temporally switching gradient field is accompanied by small terms on the orthogonal components; JEMRIS accounts for the lowest-order terms, proportional to G (2)/amplitude of static field (c.f. Eq. 2 in Bernstein et al. (8)).

Software Design

Programming Language and Libraries

JEMRIS was developed in C++ to achieve usability, as well as performance. Object-oriented design, along with code encapsulation, is utilized to keep the project maintainable and extensible. The project relies on four external libraries: First, an efficient numerical integrator was found in the CVODE library, a highly optimized variable time-stepping integrator for ordinary differential equations (9). Second, problem parallelization uses the MPI library, available on many different hardware architectures. Next, problem initialization is done with the general-purpose markup language XML through the Xerces library. XML inherently uses tree representation of data, which is of special importance for the MRI sequence. Finally, a high degree of user flexibility is employed through the GiNaC library for symbolic calculations; this approach is discussed in more detail below. A summary of the availability, purpose, and licensing of these libraries is given in Table 1. Note that all of them are open-source software.

Framework Components

A detailed description of the software framework, a hands-on user guide, and elaborate application interface program documentation are provided on the developer website of JEMRIS. Here, only a brief summary is presented to introduce the main concepts. The software roughly divides into five main classes, Sample, Signal, Model, Sequence, and Coils. The Sample and the Signal classes mobilize all functionality that is related to Input/Output (I/O) of physical data, as well as message passing for sending and receiving the data over distributed processes via the MPI standard. The Sample class describes the physical properties of the object (Eq. 4) and the Signal holds information about the MR signal (Eq. 5). The Model class mobilizes the functionality for solving the physical problem. The abstract base class is designed to communicate with the Sequence class, but no explicit solver is implemented. Currently, JEMRIS provides one explicit realization, which is the CVODE solution of the Bloch equation. Modern solvers like CVODE do not use constant time stepping. Instead, they use algorithms that continuously monitor the accuracy of the solution and adaptively change the step size to maintain a consistent level of accuracy. The high performance of CVODE to solve the Bloch equations can only be utilized if an appropriate temporal sampling of the MRI sequence is provided (see below). Further, the Model class considers two types of random fluctuations to realistically simulate MRI, as explained in the Concepts section.

The Sequence class required the most effort in terms of software design. Similar to the concept in Jochimsen and von Mengershausen (6), the sequence loop is represented as a left-right ordered tree. However, apart from the tree representation, it is most important to have software components that efficiently construct such a sequence tree. Tree nodes of a specific type are abstract base classes, so that new modules of these types are easily constructed by inheritance. This holds especially for the next four items.

Sequence XML representation. Each sequence module is uniquely represented through an XML serialization of the C++ object. Branch nodes represent loops and leaf nodes play out the actual pulses. The XML tree is parsed by the software and converted to the C++ sequence tree object.

Temporal sampling. Each module defines its own temporal sampling pattern, which may be sparse and nonequidistant. The pattern is called "time points of interest" (TPOIs); for instance, a standard trapezoidal gradient has four TPOIs: start time, end of the ramp-up, end of the flat-top, and end of the ramp-down, respectively. "Signal acquisition" periods are modeled by an array of equidistant TPOIs with a Boolean storage flag and user-defined duration and "dwell-time."

Module interaction. Parameter dependences between modules are subject to a general state observation. The mechanism is adopted from the observer design pattern (11): different parameters of different modules may observe each other. A parameter change is then automatically detected and all observing modules are notified, which triggers repreparation.

Symbolic math. Interaction of modules is analytically expressed through arbitrary user-defined equations, which are evaluated in runtime. Further, symbolic math evaluation may be mobilized for user-defined analytical

Table 1
Third party libraries used in JEMRIS

Library	Availability (URL)	General purpose	JEMRIS usage	License
MPICH	www-unix.mcs.anl.gov/mpi	HPC message parsing	Splitting of sample and collecting of results	BSD-like
Xerces-C	xerces.apache.org/xerces-c	Validating XML parser	Configuration parsing, sequence representation	Apache
CVODE	www.llnl.gov/casc/sundials	ODE solver	Numerically solving the general Bloch equations	BSD-like
GiNaC	www.ginac.de	Symbolic calculation	Symbolic module dependences evaluation	GPL

gradient and RF waveforms, as well as the spatial dependence of pulsed nonlinear gradient encoding.

The TPOI concept has two implications: first, the sampling of the complete pulse diagram is usually short. It is computed on the fly and visualized during sequence design. Second, but more important, the variable time-stepping solver CVODE is extremely accelerated since it is forced to compute solutions only at the TPOIs. The most powerful concept in terms of flexible sequence design is given by the combination of module observation and symbolic math evaluation: Via the observer design, parameters of modules may be arbitrarily linked against each other, e.g., a gradient pulse may define its area from the area of another gradient event. Since one usually would like to further mathematically manipulate such dependences, e.g., "gradient X should take half the area of gradient Y," the parameter dependences are subject to symbolic calculation with the GiNaC library. Additionally, sequence internal variables such as loop counters are observable. As a consequence, for instance, JEMRIS does not need specialized modules for phase-encoding gradient tables. Instead, an arbitrary encoding order may be directly specified by means of mathematical expressions in which loop counters are referenced. Then, the observer mechanism sets the correct gradient area dynamically in runtime. An example of the sequence tree concept and symbolic module dependences is depicted in Fig. 1. For a detailed description, the reader is referred to the JEMRIS website.

Finally, the Coil class contains the code for spatially varying RF transmission and signal reception. It derives from the same base class as the Sequence class, and thus the complete observer mechanism is available. Generally, a derived explicit Coil class needs to implement methods for receive, transmit, and obtaining its spatial sensitivity. Four coil types have been implemented: an ideal uniform coil with a flat sensitivity pattern, a Biot-Savart-type loop, an arbitrary coil with analytically user-defined sensitivity pattern, and an arbitrary coil, which depends on a user-provided binary file holding a sensitivity map.

Main Executable Program

Simplified, the mode of action of the main simulator program is as follows: a master process splits the Sample into equal portions, which are distributed to the compute node processes. Here, the Sequence returns values of all pulse axes (RF magnitudes and phases for all transmit coils plus three gradient axes) at desired time points—the TPOIs—to the Model, which numerically solves the Bloch equation individually for each spin. The Coil receives and sums the net Signal at every desired time point, which is sent back to the master process, where finally the bulk signal is summed and stored.

User Interfaces

Experience showed that acceptance of the software is increased if a GUI is provided, and data I/O are supported from Matlab[1] such that users can easily test self-written Matlab code for either sample construction or signal processing. For these reasons, three Matlab GUIs were developed: one for interactively designing the MRI sequence, another for defining the coil configuration, and one for the setup and execution of the main simulator, respectively. The latter provides some predefined samples, such as the MNI human brain phantom,[2] as well as the possibility for the input of a user-defined sample. Note that all Matlab GUIs follow the same procedure: construct a valid XML file from the user input, then call the external JEMRIS executables to compute the data, and finally read and visualize the result.

RESULTS

Performance Evaluation

All simulations were performed on a 32-dual-core CPU Opteron cluster (Advanced Micro Devices, Sunnyvale, California). This can be seen as a small-scale high-performance computing: it is, however, sufficient to perform reasonable MRI simulations of approximately 10^5 spins within minutes, depending on the MRI sequence (see examples below). Performance evaluation was carried out by simulating spatially selective excitation with large tip angles (12,13). This reflects well the capabilities of JEMRIS, i.e., the correct numerical simulation of simultaneously applied RF and gradient events. The simulation result depicted in Fig. 2a reproduces very well the original imaging experiments by Pauly et al. (13). The program profiling results in Fig. 2b show that most of the time is spent in the highly optimized CVODE libraries. However, a significant fraction of 28% is spent in retrieving the MRI sequence values. Finally Fig. 2c shows, as expected, that parallel performance scales nearly perfectly, i.e., the speed linearly increases with the number of processors. Running the same test on the campus supercomputer, JUGENE, showed that the program also scales with more than 1000 processes. To illustrate the absolute performance of JEMRIS in typical experiments of educational value, simulations of well-known MRI artifacts were performed. The corresponding

[1]http://www.mathworks.com.
[2]http://www.bic.mni.mcgill.ca/brainweb.

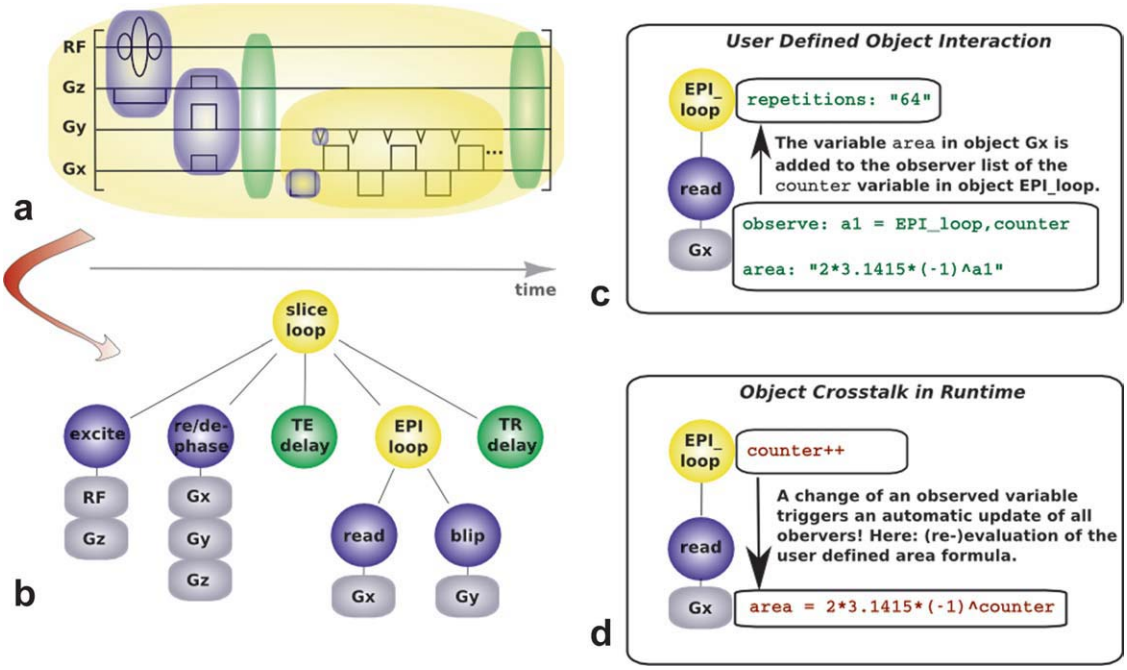

FIG. 1. **a:** Sketch of a native EPI pulse sequence diagram. **b:** Representation of the same diagram with a left-right ordered tree. Branching nodes represent loops and leaf nodes represent modules in which the actual pulse shapes are played out. **c,d:** Attribute observation mechanism: the observation of other attributes is performed via the "Observer" attribute. These quantities may then be used in any symbolic equation. Here, the dynamically polarity-switching read gradient automatically sets its area according to the formula $A = 2\pi(-1)^n$, where n is the EPI loop counter, retrieved through attribute observation. A change of the loop counter triggers an update of the gradient area.

results are shown in Fig. 3: (Fig. 3a) echo-planar imaging (EPI) simulation considering chemical shift effects yields the prominent fat-water shift in MRI. Note that an ideal homogeneous amplitude of static field was simulated so that the usual EPI distortions are not present; (Fig. 3b) malfunctioning MR scanner hardware simulation with a nonlinear gradient field results in a distorted image; (Fig. 3c) balanced Steady State Free Precession (SSFP) simulation including susceptibility-induced field inhomogeneity yields the well-known banding artifacts in the human brain; (Fig. 3d) artifact in spin-echo imaging due to a very long refocusing pulse exciting transverse magnetization. These examples can be easily reproduced with JEMRIS. Details are given on the website, where all sequence and simulation parameters are included. Here, the examples serve for a qualitative presentation of JEMRIS's capabilities.

Applications

To underline the importance and impact of MRI simulations, as well as the various possibilities to be achieved with JEMRIS, three different applications in current hot-topic research areas are presented.

Imaging With Nonlinear Spatial Encoding Fields

Curved field gradients such as the PatLoc approach (14) are currently under discussion for region-specific zoomed

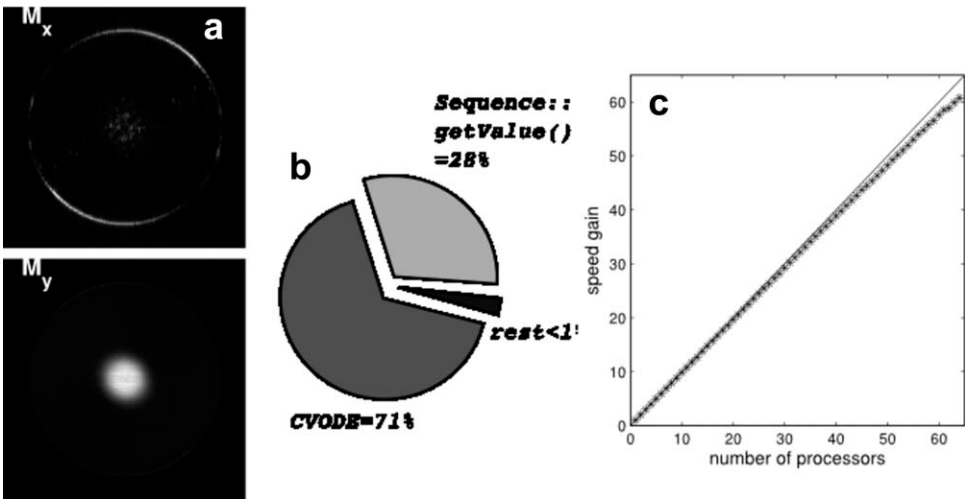

FIG. 2. JEMRIS performance evaluation by simulating a spin-echo EPI sequence with selective refocusing pulse. The simulated MR image, **(a)** (top: real part, bottom: imaginary part), reproduces very well the original imaging experiments by Pauly et al. (13). Sequential profiling **(b)** shows the efficiency of the software, which spends 71% of the computation time in the CVODE library for numerical integration. Speed gain due to parallelization **(c)** is close to the optimum (the bisecting line).

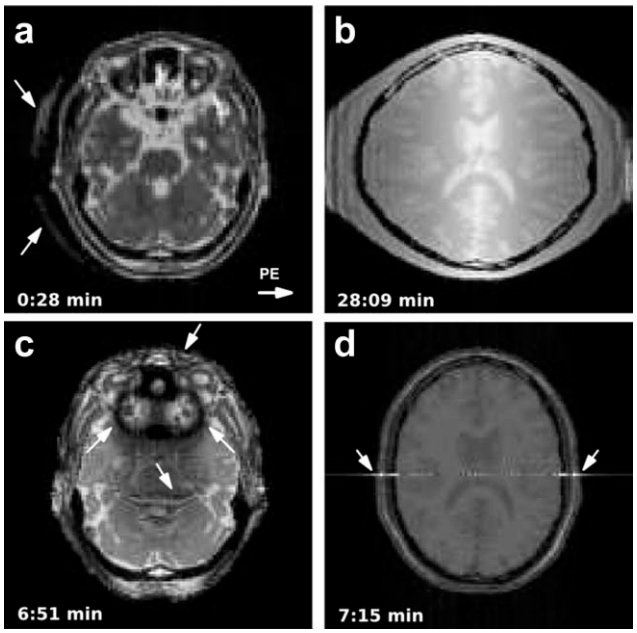

FIG. 3. MRI artifact simulations: **(a)** EPI chemical shift; **(b)** distortions due to nonlinear gradients; **(c)** balanced SSFP banding artifacts; **(d)** spin-echo imaging with a refocusing pulse duration $\approx T_2$. In all cases, $1.4 \cdot 10^5$ isochromats were simulated. The calculation times (bottom left on each image) are longer for sequences with many RF events, e.g., in **(c)** and **(d)** 128 and 256 RF pulses are applied, respectively, while just one RF pulse is performed in the EPI simulation in **(a)**. The simulation of nonlinear gradients takes longest since the software needs to perform symbolic evaluation of the user-specified spatial field dependence at the location of each isochromat.

spatial encoding with reduced hardware demand and peripheral nerve stimulations at higher switching rates. JEMRIS allows one to simulate such experiments, with few limitations on the complexity of the physical processes. For demonstration purpose, Fig. 4 depicts one-dimensional gradient-echo imaging simulations with different gradient fields: linear encoding, cubic encoding, arc-tangent encoding, and a Rayleigh function, respectively, where the latter resembles PatLoc encoding. Except for linear encoding, note the region-specific resolution properties in the one-dimensional image. Further, note that the arc-tangent is an artificial example as it does not reflect a physically feasible field with existing coil designs. Extending these simulations to two dimensions and three dimensions, as well as the incorporation of multiple RF coil sensitivities for parallel receive, is straightforward with JEMRIS.

Selective Excitation With an Array of Independently Driven Transmit Coils

Multidimensional, spatially selective excitation is an important concept of growing interest in MRI, e.g., in the field of in vivo spectroscopy or for the challenging task of correcting subject-induced amplitude of RF field inhomogeneities at ultrahigh fields (15). Figure 5 depicts the capability of JEMRIS to correctly simulate such experiments, here showing the influence of the number of transmit channels and relaxation during the pulse. The corresponding RF pulses were calculated by means of the small-tip-angle approximation for the case of parallel transmission (16). Spatial gradient encoding during the RF pulse was performed with a uniformly sampling spiral trajectory (17).

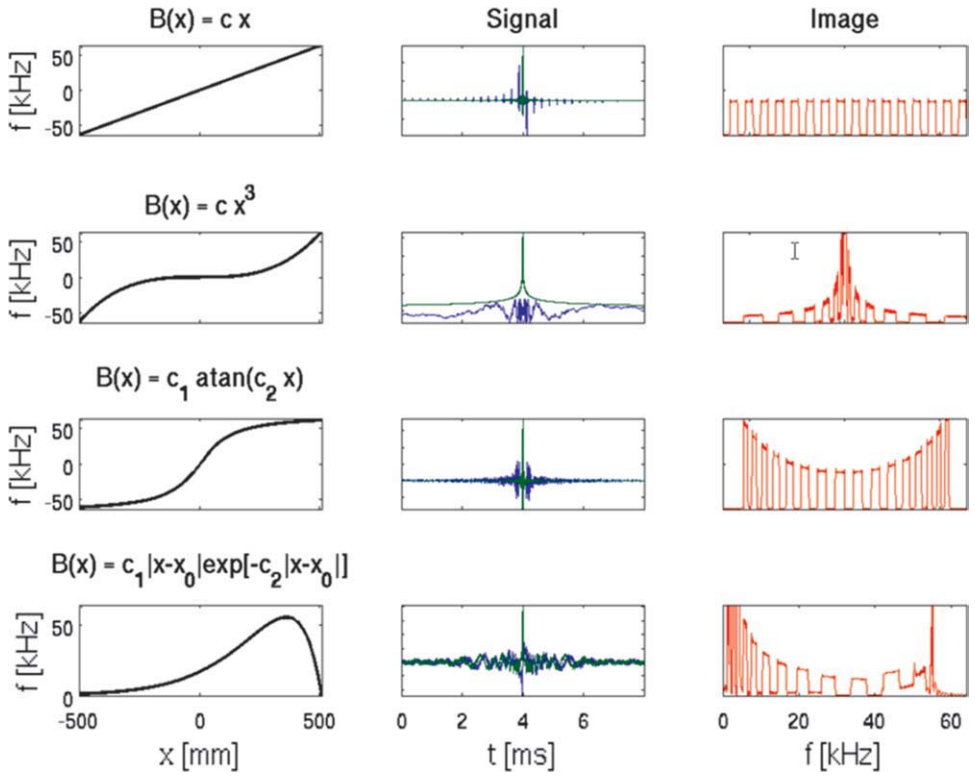

FIG. 4. One-dimensional imaging simulation of a repeated boxcar function. Position encoding with various curved magnetic fields results in region-dependent resolution properties of the encoding. Spatial encoding functions from top to bottom row: linear, cubic, arc-tangent, Rayleigh.

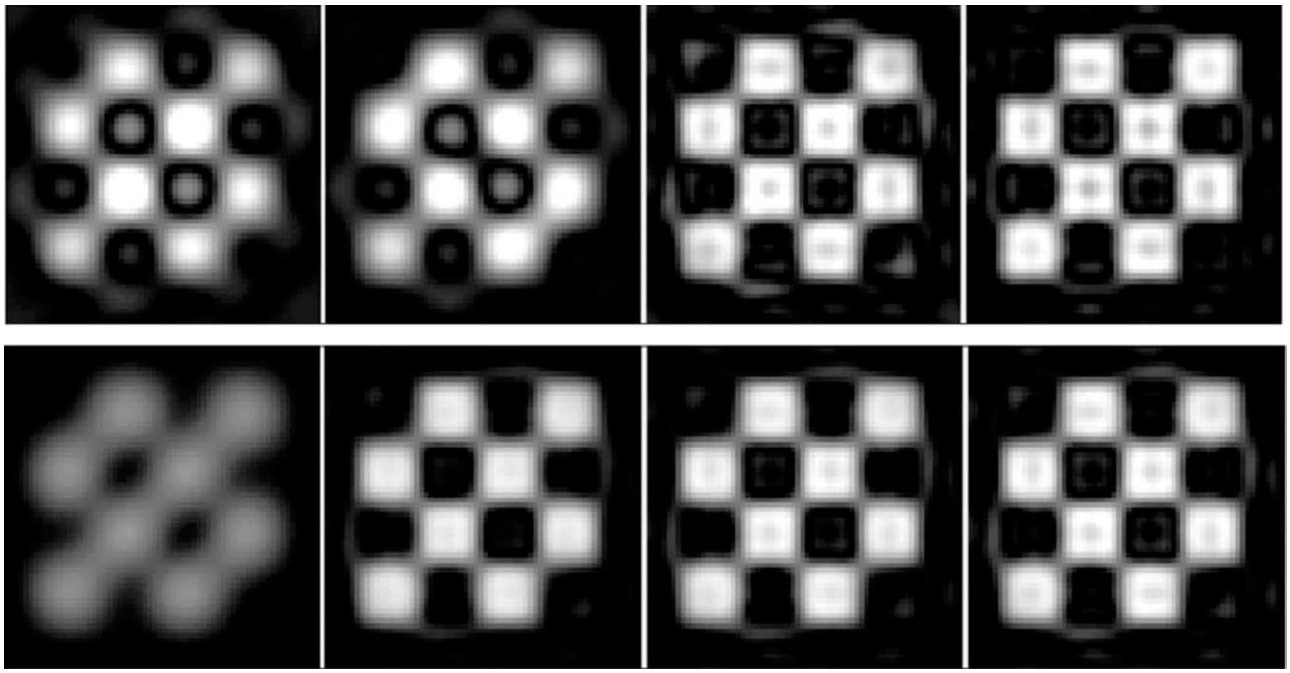

FIG. 5. Selective excitation simulation. Top row: excitation of a 64 × 64 checkerboard pattern achieved with 2-ms pulses but varying numbers of transmit channels to achieve different pattern fidelity; one, four, eight, and 16 channels were used from left right. Bottom row: same simulation but varying pulse length and a sample with low T_2^* (5 ms). Excitation was accelerated according to the transmit SENSE theory. From left to right, the pulse length were 5.12, 1.28, 0.64, and 0.32 ms.

Undersampled MRI Data in the Presence of Motion

k-t BLAST (18) is an important imaging modality for dynamic MRI. This technique acquires undersampled images at each timeframe, which are then reconstructed using compressed sensing methods. Current simulations (18,19) of k-t BLAST take into account movement between two timeframes; however, they neglect movement during the acquisition of a single timeframe. Since k-t BLAST was introduced to image rapid motion such as a beating heart, it is reasonable to assume significant motion during the acquisition of each timeframe. This effect can be investigated using JEMRIS since it is capable of simulatin moving isochromats. The result of such a study is shown in Fig. 6. An oscillating sphere with a period of T = 1 sec was simulated with (upper row) and without (lower row) motion during the acquisition. The acquisition time of a single timeframe was 40 ms, and the pulse repetition time between two timeframes was 50 ms. The additional artifacts arising from motion during the acquisition are clearly visible and can be studied using JEMRIS.

DISCUSSION

This software is first of all intended as a tool for the MRI physicist to support new investigations and inventions in the field of MRI method development. It allows for time tracking of the net magnetization, splitting of different effects, and therefore the investigation of special MR samples and new MRI sequences under a variety of

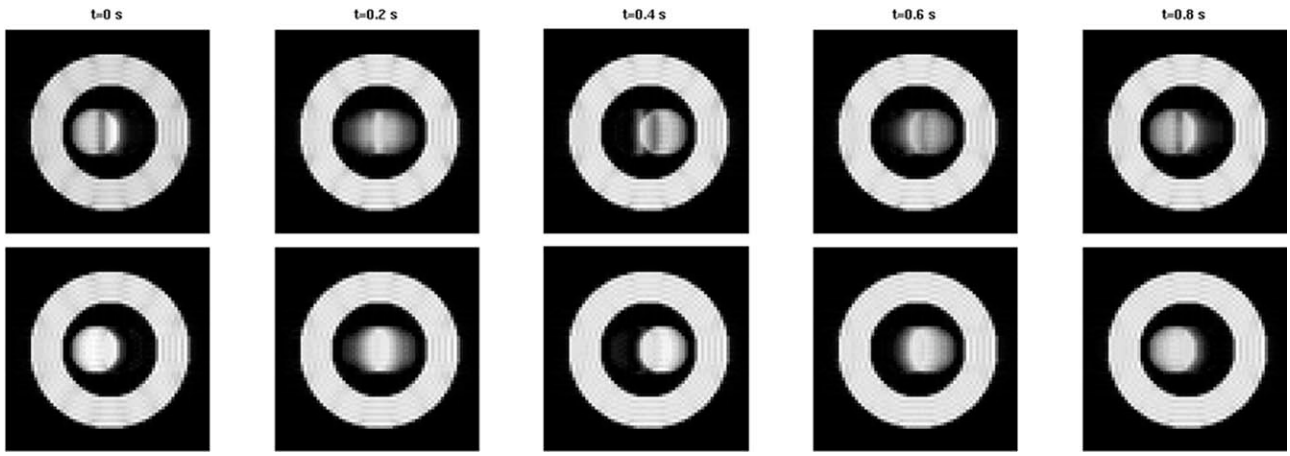

FIG. 6. k-t BLAST simulation of an oscillating sphere. Upper row: normal oscillation, lower row: no movement during acquisition, sphere jumps instantaneously to next position.

experimental conditions. Utilizing parallel computing with low communication overhead, the software perfectly scales from a single or a group of standard office personal computers up to state-of-the-art supercomputers, whereas the former is perfectly well suited for many situations. JEMRIS was developed in a lean, modular, and extensible way and is provided as an open-source project with the perspective to gain from the input of the MRI research community. Another aspect was usability: experiments may be quickly designed where no specialized knowledge apart from MRI physics is needed. This, in combination with the generality and variety of physics covered by the solver, makes the approach novel and unique in comparison to existing MRI simulators. Explicitly, the numerical integration of Eq. 3 ensures correct simulation of physics for arbitrary temporal and spatial dependence of all driving magnetic fields, as well as the object parameters. JEMRIS provides tools to model manifold spatiotemporal field and parameter variations according to Eqs. 1, 2, and 4. This combination of generality and flexibility offers the possibility to easily simulate complex MRI processes, as shown in Figs. 4, 5, and 6. Compared to JEMRIS, other common freely available MRI simulators, e.g., (1–3), have some or all of the following limitations: (i) utilizing analytical solutions of the simplified decoupled Bloch equation, (ii) no possibilities to easily investigate arbitrary complex driving magnetic fields (without programming of new sequences), (iii) limited or no spatiotemporal object variations, (iv) no parallel receive and transmit, and (v) no general description of spin dephasing within a voxel. Thus, they are well suited only in a reduced subset of numerical simulations to accurately simulate real MRI experiments.

JEMRIS also has certain limitations as physics beyond the standard Bloch equation is not yet taken into account. Further developments currently in progress are (i) Maxwell-based simulators for RF coil design; (ii) diffusion, perfusion, and brain function; (iii) multipool magnetization transfer models; and (iv) the treatment of spin 3/2 systems (sodium).

CONCLUSIONS

The open-source C++ software project JEMRIS is a versatile multiplatform MRI simulation environment and is the first simulator combining general Bloch equation-based modeling of a large spin system under the influence of the most important off-resonance effects, parallel receive and transmit, nonlinear gradient fields, and spatiotemporal parameter variations at different levels. The new sequence design paradigm provides high flexibility at low effort.

ACKNOWLEDGMENTS

This project was partly supported by the Jülich-Aachen-Research Alliance (JARA), which is funded by the Excellence Initiative of the German federal and state governments. The code for k-t BLAST reconstruction was provided by Shaihan Malik, Imperial College London. JEMRIS is available from the official developer website http://www.jemris.org. The code is distributed under the GNU General Public License as published by the Free Software Foundation, cf. http://www.gnu.org/licenses/gpl.html.

REFERENCES

1. Kwan R, Evans A, Pike G. MRI simulation-based evaluation of image-processing and classification methods. IEEE Trans Med Imaging 1999;18:1085–1097.
2. Benoit-Cattin H, Collewet G, Belaroussi B, Saint-Jalmes H, Odet C. The SIMRI project: a versatile and interactive MRI simulator. J Magn Reson 2005;173:97–115.
3. Yoder D, Zhao Y, Paschal C, Fitzpatrick J. MRI simulator with object-specific field map calculations. Magn Reson Imaging 2004;22:315–328.
4. Summers R, Axel L, Israel S. A computer simulation of nuclear magnetic resonance imaging. Magn Reson Med 1986;3:363–376.
5. Olsson M, Wirestam R, Persson B. A computer simulation program for MR imaging: application to RF and static magnetic field imperfections. Magn Reson Med 1995;34:612–617.
6. Sharp J, Yin D, Tyson R, Lo K, Tomanek B. An Integrated, Console/MR physics simulation system. 14th Meeting of the International Society for Magnetic Resonance in Medicine, Seattle, 2006.
7. Marques J, Bowtell R. Application of a Fourier-based method for rapid calculation of field inhomogeneity due to spatial variation of magnetic susceptibility. Concepts Magn Reson B 2005;25B:65–78.
8. Bernstein M, Zhou X, Polzin J, King K, Ganin A, Pelc N, Glover G. Concomitant gradient terms in phase contrast MR: analysis and correction. Magn Reson Med 1998;39:300–308.
9. Cohen S, Hindmarsh A. CVODE, a stiff/nonstiff ODE solver in C. Comput Phys 1996;10:138–143.
10. Jochimsen T, von Mengershausen M. ODIN: object-oriented development interface for NMR. J Magn Reson 2004;170:67–78.
11. Gamma E, Helm R, Johnson RE, Vlissides J. Design Patterns. Elements of Reusable Object-Oriented Software, Addison-Wesley, Boston, 1995. p 416.
12. Pauly J, Nishimura D, Macovski A. A linear class of large-tip-angle selective excitation pulses. J Magn Reson 1989;82:571–587.
13. Pauly J, Nishimura D, Macovski A. A k-space analysis of small tip-angle excitation pulses. J Magn Reson 1989;81:43–56.
14. Hennig J, Welz AM, Schultz G, Korvink J, Liu Z, Speck O, Zaitsev M. Parallel imaging in non-bijective, curvilinear magnetic field gradients: a concept study. MAGMA 2008;21:5–14.
15. Ibrahim T, Lee R, Abduljalil A, Baertlein B, Robitaille P. Dielectric resonances and b1 field inhomogeneity in UHFMRI. Magn Reson Imaging 2001;19:219–226.
16. Ullmann P, Junge S, Wick M, Seifert F, Ruhm W, Hennig J. Experimental analysis of parallel excitation using dedicated coil setups and simultaneous RF transmission on multiple channels. Magn Reson Med 2005;54:994–1001.
17. Block KT, Frahm J. Spiral imaging: a critical appraisal. J Magn Reson Imaging 2005;21:657–668.
18. Tsao J, Boesinger P, Pruessmann K. k-t BLAST and k-t SENSE: dynamic MRI with high frame rate exploiting spatiotemporal correlations. Magn Reson Med 2003;50:1031–1042.
19. Hansen M, Kozerke S, Pruessmann K, Boesinger P, Pedersen E, Tsao J. On the influence of training data quality in k-t BLAST reconstruction. Magn Reson Med 2004;52:1175–1183.